

Anytime Parallel Tempering

Alix Marie d’Avigneau^{*1}, Sumeetpal S. Singh¹, and Lawrence M. Murray²

¹Signal Processing and Communications Group, Department of Engineering, University of Cambridge

²Uber AI Labs

Abstract

Developing efficient and scalable Markov chain Monte Carlo (MCMC) algorithms is indispensable in Bayesian inference. To improve their performance, a possible solution is parallel tempering, which runs multiple interacting MCMC chains to more efficiently explore the state space. The multiple MCMC chains are advanced independently in what is known as local moves, and the performance enhancement steps are the exchange moves, where the chains pause to exchange their current sample among each other. To reduce the real time taken to perform the independent local moves, they may be performed simultaneously on multiple processors. Another problem is then encountered: depending on the MCMC implementation and the inference problem itself, the local moves can take a varying and random amount of time to complete, and there may also be computing infrastructure induced variations, such as competing jobs on the same processors, an issue one must contend with in a cloud computing setting, for example. Thus before the exchange moves can occur, all chains must complete the local move they are engaged in so as to avoid introducing, a potentially substantial, bias (Proposition 2.1). To solve this problem of randomly varying local move completion times when parallel tempering is implemented on a multi-processor computing resource, we adopt the Anytime Monte Carlo framework of Murray et al. [2016]: we impose real-time deadlines on the parallelly computed local moves and perform exchanges at these deadline without any processor idling. We show our methodology for exchanges at real-time deadlines does not introduce a bias and leads to significant performance enhancements over the naïve approach of idling until every processor’s local moves complete.

Keywords : Bayesian inference, Markov chain Monte Carlo (MCMC), Parallel Tempering, Anytime Monte Carlo, Approximate Bayesian computation, Likelihood-free inference.

1 Introduction

Consider a set of m observations $y = \{y_1, \dots, y_m\} \in \mathcal{Y}$ following a probability model with underlying parameters $\theta \in \Theta$ and associated *likelihood* $f(y_1, \dots, y_m | \theta)$ which we abbreviate to $f(y | \theta)$. In most cases, the posterior $\pi(d\theta)$ of interest is intractable and must be approximated using computational tools such as the commonly used *Metropolis-Hastings* (M-H) algorithm (Robert and Casella [2004]) with random walk proposals, for example. However, as models become more complex, the exploration of the posterior using such basic methods quickly becomes inefficient (Beskos et al. [2009]). Furthermore, the model itself can pose its own challenges such as the likelihood becoming increasingly costly or even impossible to evaluate (Tavaré et al. [1997]); the Lotka-Volterra predator-prey model of Section 5 is a concrete example.

*A. Marie d’Avigneau is supported by the UK Engineering and Physical Sciences Research Council (EPSRC).

Parallel tempering, initially proposed by Swendsen and Wang [1986] and further developed under the name Metropolis-coupled Markov chain Monte Carlo (MC)³ by Geyer [1991], is a generic method for improving the efficiency of MCMC that can be very effective without altering the original MCMC algorithm, for example by designing more efficient proposals. The parallel tempering algorithm runs multiple interacting MCMC chains to more efficiently explore the state space. The multiple MCMC chains are advanced independently, in what is known as the local moves, and the performance enhancement steps are the exchange moves, where the chains pause and attempt to swap their current sample amongst each other. Parallel tempering allows for steps of various sizes to be made when exploring the parameter space, which makes the algorithm effective, even when the distribution we wish to sample from has multiple modes. In order to reduce the real time taken to perform the independent local moves, they may be performed simultaneously on multiple processors, a feature we will focus on in this work.

Let the parallel tempering MCMC chain be $(X_n^{1:\Lambda})_{n=1}^\infty = (X_n^1, \dots, X_n^\Lambda)_{n=1}^\infty$ with initial state $(X_0^{1:\Lambda})$ and target distribution

$$\pi(dx^{1:\Lambda}) \propto \prod_{\lambda=1}^{\Lambda} \pi_\lambda(dx^\lambda) \quad (1)$$

where the $\pi_\lambda(\cdot)$ are independent marginals corresponding to the target distribution of each of Λ chains, running in parallel at different temperatures indexed by λ . One of these chains, say $\lambda = \Lambda$, is the *cold* chain, and its target distribution $\pi_\Lambda = \pi$ is the posterior of interest. At each step n of parallel tempering (Geyer [2011]), one of two types of updates is used to advance the Markov chain $X_n^{1:\Lambda}$ to its next state:

1. Independent *local moves*: for example, a standard Gibbs or Metropolis-Hastings update, applied to each tempered chain X_n^λ in parallel.
2. Interacting *exchange moves*: propose to swap the states $x \sim \pi_\lambda$ and $x' \sim \pi_{\lambda'}$ of one or more pairs of adjacent chains. For each pair, accept a swap with probability

$$\min \left\{ 1, \frac{\pi_\lambda(x')\pi_{\lambda'}(x)}{\pi_\lambda(x)\pi_{\lambda'}(x')} \right\} \quad (2)$$

otherwise, the chains in the pair retain their current states.

With the cold chain providing the desired precision and the warmer chains more freedom of movement when exploring the parameter space, the combination of the two types of update allows all chains to mix much faster than any one of them would mix on its own. This provides a way to jump from mode to mode in far fewer steps than would be required under a standard non-tempered implementation using, say, the Metropolis-Hastings algorithm.

A particular advantage of parallel tempering is that it is possible to perform the independent local moves in parallel on multiple processors in order to reduce the real time taken to complete them. Unfortunately, this gives rise to the following problem: depending on the MCMC implementation and the inference problem itself, the local moves can take a *varying and random* amount of time to complete, which depends on the part of the state space it is exploring. (See the Lotka-Volterra predator-prey model in Section 5 for a specific real example.) Thus, before the exchange moves can occur, all chains *must* complete the local move they are engaged in to avoid introducing a potentially substantial bias (see Proposition 2.1). Additionally, the time taken to complete local moves may also reflect computing infrastructure induced variations, for example, due to variations in processor hardware, memory bandwidth, network traffic, I/O load, competing jobs on the same

processors as well as potential unforeseen interruptions due to e.g. system failures, all of which affect the compute time of local moves. The contributions of this paper are as follows.

Firstly, to solve the problem of randomly distributed local move completion times when parallel tempering is implemented on a multi-processor computing resource, we adopt the Anytime Monte Carlo framework of [Murray et al. \[2016\]](#): we guarantee the simultaneous readiness of all chains by imposing real-time deadlines on the parallelly computed local moves, and perform exchange moves at these deadline without any idling, i.e. without waiting for the slowest of them to complete their local moves. Idling is both a financial cost, for example in a cloud computing setting, and can also significantly reduce the effective Monte Carlo sample size returned. We show that hard deadlines introduce a bias which we mitigate using the Anytime framework (see [Proposition 3.1](#)). We illustrate our gains through detailed numerical work.

Secondly, we perform a detailed numerical study of the Lotka-Volterra predator-prey model where local moves take a varying and random amount of time to complete depending on the part of the state space the Markov chain is exploring. The likelihood cannot be evaluated and a simulation-based approach known as Approximate Bayesian computation ([Tavaré et al. \[1997\]](#), [Pritchard et al. \[1999\]](#)) developed in [Lee \[2012\]](#) is adopted. In [Lee \[2012\]](#), an efficient rejection-style MCMC kernel known as the *1-hit MCMC kernel* was developed in which a ‘race’ takes place when new candidate samples are proposed. The duration of the race depends on the likelihood of the candidate parameter samples. In this paper, we show we can improve the performance of the 1-hit MCMC kernel by introducing tempering and exchange moves, and apply the resulting parallel tempering algorithm within the Anytime framework.

This paper is structured as follows. [Sections 2 and 3](#) develop our Anytime Parallel Tempering Monte Carlo (APTMC) algorithm and then [Section 4](#) extends our framework further for the 1-hit MCMC kernel of [Lee \[2012\]](#) for approximate Bayesian computation. Experiments are run in [Section 5](#) and include a carefully constructed synthetic example to demonstrate the workings and salient features of Anytime parallel tempering. [Section 5](#) also presents an application of Anytime parallel tempering to the problem of estimating the parameters of a stochastic Lotka-Volterra predator-prey model. Finally, [Section 6](#) provides a summary and some concluding remarks.

2 Anytime Monte Carlo

Let $(X_n)_{n=0}^\infty$ be a Markov chain with initial state X_0 , evolving on state space \mathcal{X} , with transition kernel $X_n | x_{n-1} \sim \kappa(dx_n | x_{n-1})$ and target distribution $\pi(dx)$. Define the *hold time* H_{n-1} as the random and positive real time required to complete the computations necessary to transition from state X_{n-1} to X_n via the kernel κ . Then let $H_{n-1} | x_{n-1} \sim \tau(dh_{n-1} | x_{n-1})$ where τ is the hold time distribution.

Assume that the hold time $H > \epsilon > 0$ for minimal time ϵ , $\sup_{x \in \mathcal{X}} \mathbb{E}[H | x] < \infty$, and the hold time distribution τ is homogeneous in time. In general, nothing is known about the hold time distribution τ except how to sample from it, i.e. by recording the time taken by the algorithm to simulate $X_n | x_{n-1}$. Let $\kappa(dx_n, dh_{n-1} | x_{n-1}) = \kappa(dx_n | h_{n-1}, x_{n-1})\tau(dh_{n-1} | x_{n-1})$ be a joint kernel. Clearly, the transition kernel $\kappa(dx_n | x_{n-1})$ is the marginal of the joint kernel over all possible hold times H_{n-1} . Denote by $(X_n)_{n=0}^\infty$ and $(H_n)_{n=0}^\infty$ the states and hold times of the joint process, and define the *arrival time* of the n -th state as

$$A_n := \sum_{i=0}^{n-1} H_i, \quad n \geq 1$$

where $a_0 := 0$. A possible realisation of the joint process is illustrated in [Figure 1](#).

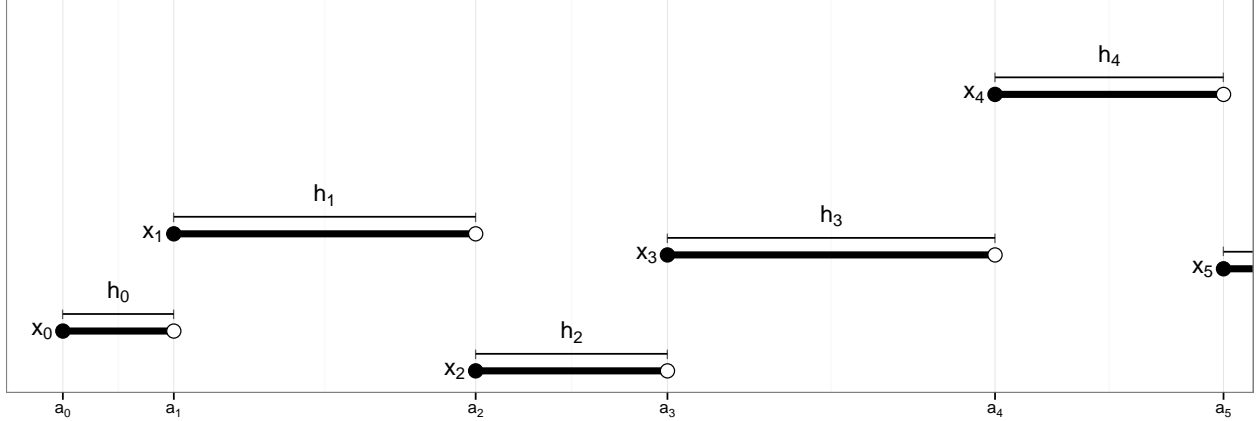


Figure 1: (Murray et al. [2016], Figure 1) Real-time realisation of a Markov chain with states $(X_n)_{n=0}^{\infty}$, arrival times $(A_n)_{n=0}^{\infty}$ and hold times $(H_n)_{n=0}^{\infty}$.

Let the process $N(t) := \sup \{n : A_n \leq t\}$ count the number of arrivals by time t . From this, construct a continuous Markov jump process $(X, L)(t)$ where $X(t) := X_{N(t)}$ and $L(t) := t - A_{N(t)}$ is the *lag time* elapsed since the last jump. This continuous process describes the progress of the computation in real time.

Proposition 2.1 (Murray et al. [2016], Proposition 1) *The continuous Markov jump process $(X, L)(t)$ has stationary distribution given by*

$$\alpha(dx, dl) = \frac{\bar{F}_\tau(l|x)}{\mathbb{E}[H]} \pi(dx) dl \quad (3)$$

where $\bar{F}_\tau(l|x) = 1 - F_\tau(l|x)$, and $F_\tau(l|x)$ is the cumulative distribution function (cdf) of $\tau(dh_n|x_n)$.

Corollary 2.1 (Murray et al. [2016], Corollary 2) *The marginal $\alpha(dx)$ of the density in Equation 3 is length-biased with respect to the target density $\pi(dx)$ by expected hold time, i.e.*

$$\alpha(dx) = \frac{\mathbb{E}[H|x]}{\mathbb{E}[H]} \pi(dx) \quad (4)$$

The proofs of Proposition 2.1 and Corollary 2.1 are given in Murray et al. [2016].

The distribution α is referred to as the *anytime distribution* and is the stationary distribution of the Markov jump process. Note that Proposition 2.1 suggests that when the real time taken to draw a sample depends on the state of the Markov chain, i.e. $\mathbb{E}[H|x] \neq \mathbb{E}[H]$, a length bias with respect to computation time is introduced. In other words, when interrupted at real time t , the state of a Monte Carlo computation targeting π is distributed according to the anytime distribution α , which can essentially be seen as a length-biased target distribution. This bias diminishes with time, and when an empirical approximation or average over all post burn-in samples is required, it may be rendered negligible for a long enough computation. However, the bias in the final state does not diminish with time, and when this final state is important – which is the case in parallel tempering – the bias cannot be avoided by running the algorithm for longer. We now discuss the approach in Murray et al. [2016] to correct this bias. The main idea is to make it so expected hold time is independent of X , which leads to $\mathbb{E}[H|x] = \mathbb{E}[H]$ and hence $\alpha(dx) = \pi(dx)$, following Corollary 2.1. This is trivially the case for iid sampling as $\kappa(dx|x_{n-1}) = \pi(dx)$, so the hold time

H_{n-1} for X_{n-1} is the time taken to sample $X_n \sim \pi(dx)$, and therefore independent of the state X_{n-1} . One approach to non-iid sampling involves simulating $K+1$ Markov chains for $K > 0$, where we assume for now that all the Markov chains are targeting π and using the same transition kernel κ and hold time distribution τ . By simulating these $K+1$ chains on the same processor in a serial schedule, we ensure that whenever the real-time deadline t is reached, states from all but one of the chains, say the $(K+1)$ -th chain, are independently distributed according to the target π . Since the $(K+1)$ -th chain is the currently working chain, i.e. the latest to go through the simulation process, its state at the real-time deadline is distributed according to the anytime distribution α . Simply discarding or ignoring the state of this $(K+1)$ -th chain eliminates the length bias. See [Murray et al. \[2016\]](#) (Section 2.1) for more details.

Using this multiple chain construction, it is thus possible draw samples from π by interrupting the process at any time t . This sets the basis for the focus of this paper: the Anytime Parallel Tempering Monte Carlo (APTMC) algorithm, described next.

3 Anytime Parallel Tempering Monte Carlo (APTMC)

3.1 Overview

Consider the problem in which we wish to sample from target distribution $\pi(dx)$. In a parallel tempering framework, construct Λ Markov chains where each individual chain λ targets the tempered distribution

$$\pi_\lambda(dx) = \pi(dx)^{\frac{\lambda}{\Lambda}}$$

and is associated with kernel $\kappa_\lambda(dx_n | dx_{n-1})$ and hold time distribution $\tau_\lambda(dh_n | x_n)$. Assume that all Λ chains are running concurrently on Λ processors. We aim to interrupt the computations on a real-time schedule of times t_1, t_2, t_3, \dots to perform exchange moves between adjacent pairs of chains before resuming the local moves. To illustrate the challenge of this task, we discuss the case where $\Lambda = 2$. Let π_2 be the desired posterior and π_1 the ‘warm’ chain, with associated hold time distributions τ_1 and τ_2 , respectively. When the two chains are interrupted at some time t , assume that the current sample on chain 1 is X_m^1 and that of chain 2 is X_n^2 . It follows from [Corollary 2.1](#) that

$$X_m^1 \sim \alpha_1(dx) = \frac{\mathbb{E}[H_1 | x]}{\mathbb{E}[H_1]} \pi_1(dx) \neq \pi_1(dx)$$

and similarly for X_n^2 . Clearly, exchanging the samples using the acceptance probability in [Equation 2](#) is incorrect. Indeed, exchanging using the current samples X_m^1 and X_n^2 , if accepted, will result in the sample sets $\{X_1^1, X_2^1, \dots\}$ and $\{X_1^2, X_2^2, \dots\}$ being corrupted with samples which arise from their respective length-biased, anytime distributions α_1 and α_2 , as opposed to being exclusively from π_1 and π_2 . Furthermore, the expressions for α_1 and α_2 will most often be unavailable, since their respective hold time distributions τ_1 and τ_2 are not explicitly known but merely implied by the algorithm used to simulate the two chains. Finally, we could wait for chains 1 and 2 complete their computation of X_{m+1}^1 and X_{n+1}^2 respectively, and then accept/reject the exchange $(X_{m+1}^1, X_{n+1}^2) \rightarrow (X_{n+1}^2, X_{m+1}^1)$ according to [Equation 2](#). This approach won’t introduce a bias but can result in one processor idling while the slower computation finishes. We show this can result in significant idling in numerical examples.

In the next section, we describe how to correctly implement exchange moves within the Anytime framework.

3.2 Anytime exchange moves

Here, we adapt the multi-chain construction devised to remove the bias present when sampling from Λ Markov chains, where each chain λ targets the distribution π_λ for $\lambda = 1, \dots, \Lambda$. Associated with each chain is MCMC kernel $\kappa_\lambda(dx_n^\lambda | dx_{n-1}^\lambda)$ and hold time distribution $\tau_\lambda(dh | x)$.

Proposition 3.1 *Let $\pi_\lambda(dx)$, $\lambda = 1 \dots, \Lambda$ be the stationary distributions of Λ Markov chains with associated MCMC kernels $\kappa_\lambda(dx_n^\lambda | dx_{n-1}^\lambda)$ and hold time distributions $\tau_\lambda(dh | x)$. Assume the chains are updated sequentially and let j be the index of the currently working chain. The joint anytime distribution is the following generalisation of Proposition 2.1*

$$A(dx^{1:\Lambda}, dl, j) = \frac{1}{\Lambda} \frac{\mathbb{E}[H | j]}{\mathbb{E}[H]} \alpha_j(dx^j, dl) \prod_{\lambda=1, \lambda \neq j}^{\Lambda} \pi_\lambda(dx^\lambda)$$

The proof of Proposition 3.1 is a straightforward adaptation of the proof of Proposition 5 in Murray et al. [2016]. Conditioning on x^j , j and l we obtain

$$A(dx^{1:\Lambda \setminus j} | x^j, l, j) = \prod_{\lambda=1, \lambda \neq j}^{\Lambda} \pi_\lambda(dx^\lambda) \quad (5)$$

Therefore, if exchange moves on the conditional $A(dx^{1:\Lambda \setminus j} | x^j, l, j)$ are performed by ‘eliminating’ the j -th chain to obtain the expression in Equation 5, they are being performed involving only chains distributed according to their respective targets π_λ and thus the bias is eliminated.

3.3 Implementation

3.3.1 One processor

On a single processor, the algorithm may proceed as in Algorithm 1, where in Step 3 the Λ chains are simulated one at a time in a serial schedule. Figure 2 provides an illustration of how the algorithm works.

Algorithm 1 Anytime Parallel Tempering Monte Carlo on one processor (APTMC-1)

- 1: Initialise real-time Markov jump process $(X^{1:\Lambda}, L, J)(0) = (x_0^{1:\Lambda}, 0, 1)$
 - 2: **for** $i = 1, 2, \dots$ **do**
 - 3: Simulate real-time Markov jump process $(X^{1:\Lambda}, L, J)(t)$ until real time t_i
 - 4: Perform exchange steps on the conditional in Equation 5
 - 5: **end for**
-

3.3.2 Multiple processors

When multiple processors are available, the Λ chains may be run in parallel. However, running a single chain on each processor means that when the real-time deadline occurs, all chains will be distributed according to their respective anytime distributions α^λ , and thus be biased as exchange moves occur. Therefore, all processors must contain at least two chains. The implementation is defined as described in Algorithm 2. Each worker uses $K > 2$ chains where either all chains have the same target distribution, e.g. for $W = \Lambda$ workers, worker $w = \lambda$ contains K chains targeting π_λ , or each chain has a different target distribution. For example, with $W = \frac{\Lambda}{2}$ workers, worker w

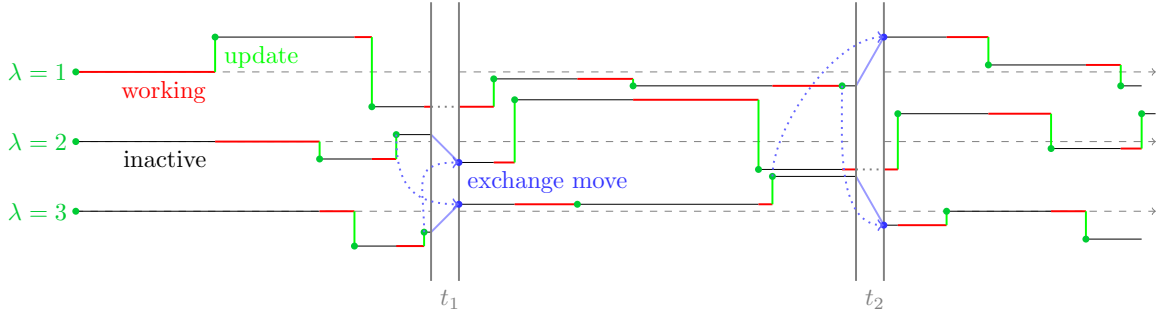


Figure 2: Illustration of the progression of three chains in the APTMC algorithm on a single processor. The *green* (local move) and *blue* (exchange move) dots represent samples from the posterior being recorded as their respective local and exchange moves are completed. When exchange moves occur at t_1 , chain $\lambda = 1$ is currently moving cannot participate in exchange moves without introducing a bias. Therefore it is ignored, and the exchange moves are performed on the remaining (inactive) chains. Similarly, a time t_2 chain $\lambda = 2$ is excluded from the exchange. The widths of intervals t_1 and t_2 are for illustrating the exchange procedure only.

could contain two chains, one with target π_w and one with target π_{2w} , or alternatively one with target π_{2w-1} and one with target π_{2w} . Note that the multiple chain construction eliminates the intractable densities in the acceptance ratio for the exchange step when τ differs between processors.

Algorithm 2 Anytime Parallel Tempering Monte Carlo on multiple processors (APTMC-W)

- 1: On worker w , initialise the real-time Markov jump process $(X_w^{1:K}, L_w, J_w)(0) = (x_0^{1:K}, 0, 1)$
- 2: **for** $i = 1, 2, \dots$ **do**
- 3: On each worker, simulate the real-time Markov jump process $(X_w^{1:K}, L_w, J_w)(t)$ until real time t_i
- 4: Across all workers, perform exchange steps on the conditional

$$A(\mathbf{d}\mathbf{x}^{1:K \setminus j} | \mathbf{x}^j, \mathbf{l}, \mathbf{j}) = \prod_{w=1}^W \prod_{k=1, k \neq j_w}^K \pi_w(\mathrm{d}x_w^k)$$

where $\mathbf{d}\mathbf{x}^{1:K \setminus j} = (\mathrm{d}x_1^{1:K \setminus j_1}, \dots, \mathrm{d}x_W^{1:K \setminus j_W})$, $\mathbf{x}^j = (x_1^{j_1}, \dots, x_W^{j_W})$, $\mathbf{l} = l_{1:W}$ and $\mathbf{j} = j_{1:W}$

- 5: **end for**
-

4 Application to Approximate Bayesian Computation

In this section we adapt the APTMC framework to approximate Bayesian computation.

4.1 Overview of Approximate Bayesian Computation

The notion of approximate Bayesian computation was developed by [Tavaré et al. \[1997\]](#) and [Pritchard et al. \[1999\]](#). It can be seen as a likelihood-free way to perform Bayesian inference, using

instead simulations from the model or system of interest, and comparing them to the observations available.

Let $y \in \mathbb{R}^d$ be some data with underlying unknown parameters $\theta \sim p(d\theta)$, where $p(\theta)$ denotes the prior for $\theta \in \Theta$. Suppose we are in the situation in which the likelihood $f(y|\theta)$ is either intractable or too computationally expensive, which means that MCMC cannot be performed as normal. Assuming that it is possible to sample from the density $f(\cdot|\theta)$ for all $\theta \in \Theta$, approximate the likelihood by introducing an artificial likelihood f^ε of the form

$$f^\varepsilon(y|\theta) = \text{Vol}(\varepsilon)^{-1} \int_{B_\varepsilon(y)} f(x|\theta) dx \quad (6)$$

where $B_\varepsilon(y)$ denotes a metric ball centred at y of radius $\varepsilon > 0$ and $\text{Vol}(\varepsilon)$ is its volume. The resulting approximate posterior is given by

$$p^\varepsilon(\theta|y) = \frac{p(\theta)f^\varepsilon(y|\theta)}{\int p(\vartheta)f^\varepsilon(y|\vartheta)d\vartheta}$$

The likelihood $f^\varepsilon(y|\theta)$ cannot be evaluated either, but a MCMC kernel can be constructed to obtain samples from the approximate posterior $\pi^\varepsilon(\theta, x)$ defined as

$$\pi^\varepsilon(\theta, x) = p^\varepsilon(\theta, x|y) \propto p(\theta)f(x, \theta)\mathbb{1}_\varepsilon(x)\text{Vol}(\varepsilon)^{-1}$$

where $\mathbb{1}_\varepsilon(x)$ is the indicator function for $x \in B_\varepsilon(y)$. This is referred to as *hitting* the ball $B_\varepsilon(y)$. In the MCMC kernel, one can propose $\theta' \sim q(d\theta'|\theta)$ for some proposal density q , simulate the dataset $x \sim f(dx|\theta')$ and accept θ' as a sample from the posterior if $x \in B_\varepsilon(y)$.

The *1-hit MCMC kernel*, proposed by Lee [2012] and described in Algorithm 3 introduces local moves in the form of a ‘race’: given current and proposed parameters θ and θ' , respectively simulate corresponding datasets x and x' sequentially. The state associated with the first dataset to hit the ball $B_\varepsilon(y)$ ‘wins’ and is accepted as the next sample in the Markov chain. The proposal θ' is also accepted as if both x and x' hit the ball at the same time.

4.2 Anytime Parallel Tempering Monte Carlo for Approximate Bayesian Computation (ABC-APTMC)

Including the 1-hit kernel in the local moves of a parallel tempering algorithm is straightforward. Exchange moves must however be adapted to this new likelihood-free setting. Additionally, the race that occurs takes a random time to complete, thus providing good motivation for the use of Anytime Monte Carlo.

4.2.1 Exchange moves

Let (θ, x) and (θ', x') be the states of two chains targeting π^ε and $\pi^{\varepsilon'}$, respectively, where $\varepsilon' > \varepsilon$. Here, this is equivalent to saying θ' is the state of the ‘warmer’ chain. We already know that x' falls within ε' of the observations y , i.e. $x' \in B_{\varepsilon'}(y)$. Similarly, we also know that $x \in B_\varepsilon(y)$, and clearly that $x \in B_{\varepsilon'}(y)$. If x' also falls within ε of y , then swap the states, otherwise do not swap. The odds ratio is

$$\frac{\pi^{\varepsilon'}(\theta, x)\pi^\varepsilon(\theta', x')}{\pi^\varepsilon(\theta, x)\pi^{\varepsilon'}(\theta', x')} = \frac{p(\theta)f(x|\theta)\text{Vol}(\varepsilon')p(\theta')f(x'|\theta')\mathbb{1}_\varepsilon(x')\text{Vol}(\varepsilon)}{p(\theta)f(x|\theta)\text{Vol}(\varepsilon)p(\theta')f(x'|\theta')\text{Vol}(\varepsilon')} = \mathbb{1}_\varepsilon(x')$$

so the probability of the swap being accepted is the probability of x' also hitting the ball of radius ε centred at y . This type of exchange move is summarised in Algorithm 4.

Algorithm 3 1-hit MCMC kernel for approximate Bayesian computation

Given current state (θ_n, x_n)

- 1: **for** $i := 1, 2, \dots$ **do**
- 2: Propose $\theta' \sim q(d\theta | \theta_n)$ \triangleright propose a local move
- 3: Compute preliminary acceptance probability \triangleright prior check

$$a(\theta_n, \theta') = \min \left\{ 1, \frac{p(\theta')q(\theta_n | \theta')}{p(\theta_n)q(\theta' | \theta_n)} \right\}$$

- 4: Sample $u \sim \text{Uniform}(0, 1)$
 - 5: **if** $u < a(\theta_n, \theta')$ **then**
 - 6: RACE := TRUE
 - 7: **else**
 - 8: RACE := FALSE
 - 9: retain $(\theta_{n+1}, x_{n+1}) = (\theta_n, x_n)$ \triangleright reject θ' as it is unlikely to win race
 - 10: **end if**
 - 11: **while** RACE **do**
 - 12: Simulate $x \sim f(dx | \theta_n)$ and $x' \sim f(dx' | \theta')$
 - 13: **if** $x \in B_\varepsilon(y)$ **or** $x' \in B_\varepsilon(y)$ **then** \triangleright stop the race once either x or x' hits the ball
 - 14: RACE := FALSE
 - 15: **end if**
 - 16: **end while**
 - 17: **if** $x' \in B_\varepsilon(y)$ **then** \triangleright accept or reject move
 - 18: set $(\theta_{n+1}, x_{n+1}) = (\theta', x')$
 - 19: **else**
 - 20: retain $(\theta_{n+1}, x_{n+1}) = (\theta_n, x)$
 - 21: **end if**
 - 22: $n := n + 1$
 - 23: **end for**
-

4.2.2 Implementation

The full implementation of the ABC-APTMC algorithm on a single processor (ABC-APTMC-1) is described in Algorithm 5. The multi-processor algorithm can similarly be modified to reflect these new exchange moves and the resulting algorithm is referred to as ABC-APTMC-W.

Algorithm 4 ABC: exchange move between two chains

Given $\omega_n = ((\theta, x), (\theta', x'))$ where $\theta \sim \pi$, $x \sim f(dx | \theta)$ and $\theta' \sim \pi'$, $x' \sim f(dx' | \theta')$.
 \triangleright both (θ, x) and (θ', x') are outputs from Algorithm 3 for different $\varepsilon' > \varepsilon$

- 1: **if** $x' \in B_\varepsilon(y)$ **then** \triangleright accept or reject swap depending on whether x' also hits the ball of radius ε
- 2: set $\omega_{n+1} = ((\theta', x'), (\theta, x))$
- 3: **else**
- 4: retain $\omega_{n+1} = \omega_n$
- 5: **end if**
- 6: $n := n + 1$

Algorithm 5 ABC: Anytime Parallel Tempering Monte Carlo Algorithm (ABC-APTMC-1)

- 1: Initialise the real-time Markov jump process $(\theta^{1:\Lambda}, L, J) = (\theta_0^{1:\Lambda}, 0, 1)$.
- 2: Set $n := 0$
- 3: **for** $i := 1, 2, \dots$ **do**
 SIMULATE THE REAL-TIME MARKOV JUMP PROCESS $(\theta, L, J)(t)$ UNTIL REAL TIME t_i
- 4: Perform local moves on (θ_n^j, x_n^j) according to Algorithm 3.
- 5: $j := j + 1$
- 6: **if** $j > \Lambda$ **then**
- 7: $j := 1$
- 8: **end if**
- PERFORM EXCHANGE STEPS ON THE CONDITIONAL:
- $$A(d\theta^{1:\Lambda} | \theta^j, l, j) = \prod_{\lambda=1, \lambda \neq j}^{\Lambda} \pi_\lambda(d\theta^\lambda)$$
- 9: Perform exchange moves on $\omega_n = ((\theta_n^\lambda, x_n^\lambda), (\theta_n^{\lambda'}, x_n^{\lambda'}))$ according to Algorithm 4.
- 10: **end for**

5 Experiments

In this section, we first illustrate the workings of the algorithms presented in Section 3.3 on a simple model, in which real-time behaviour is simulated using virtual time and an artificial hold distribution. The model is also employed to demonstrate the gain in efficiency provided by the inclusion of exchange moves. Then, the approximate Bayesian computation version of the algorithms, as presented in Section 4, is applied to two case studies. The first case is a simple model and serves to verify the workings of the approximate Bayesian computation algorithm, including bias correction. The second case considers the problem of estimating the parameters of a stochastic Lotka-Volterra predator-prey model – in which the likelihood is unavailable – and serves to

evaluate the performance of the Anytime parallel tempering version of the ABC-MCMC algorithm, as opposed to the standard versions (with and without exchange moves) on both a single and multiple processors. The exchange moves are set up so that multiple pairs could be swapped at each iteration. All experiments in this paper were run on MATLAB and the code is available at <https://github.com/alixma/ABCAPTMC.git>.

5.1 Toy example: Gamma mixture model

In this example we attempt to sample from an equal mixture of two Gamma distributions using the APTMC algorithm. Define the target $\pi(dx)$ and an ‘artificial’ hold time $\tau(dh | x)$ distributions as follows:

$$\begin{aligned} X &\sim \phi \text{Gamma}(k_1, \theta_1) + (1 - \phi) \text{Gamma}(k_2, \theta_2) \\ H | x &\sim \psi \text{Gamma}\left(\frac{x^p}{\theta_1}, \theta_1\right) + (1 - \psi) \text{Gamma}\left(\frac{x^p}{\theta_2}, \theta_2\right) \end{aligned}$$

with mixture coefficients $\phi = \frac{1}{2}$ and ψ , where $\text{Gamma}(\cdot, \cdot)$ denotes the probability density function of a Gamma distribution, with shape and scale parameters (k_1, θ_1) and (k_2, θ_2) for each components, respectively, and with polynomial degree p , assuming it remains constant for both components of the mixture.

In the vast majority of experiments, the explicit form of the hold time distribution τ is not known, but observed in the form of the time taken by the algorithm to simulate X . For this example, so as to avoid external factors such as competing jobs affecting the hold time, we assume an explicit form for τ is known and simulate virtual hold times. This consists of simulating a hold time $h \sim \tau(dh | x)$ and advancing the algorithm forward for h steps without updating the chains, effectively ‘pausing’ the algorithm. These virtual hold times are introduced such that what in a real-time example would be the effects of constant ($p = 0$), linear ($p = 1$), quadratic ($p = 2$) and cubic ($p = 3$) computational complexity can be studied. Another advantage is that the anytime distribution $\alpha_\Lambda(dx)$ of the cold chain can be computed analytically and is the following mixture of two Gamma distributions

$$\alpha_\Lambda(dx) = \varphi(p, k_1, k_2, \theta_1, \theta_2) \text{Gamma}(k_1 + p, \theta_1) + [1 - \varphi(p, k_1, k_2, \theta_1, \theta_2)] \text{Gamma}(k_2 + p, \theta_2) \quad (7)$$

where

$$\varphi(p, k_1, k_2, \theta_1, \theta_2) = \left(1 + \frac{\Gamma(k_1)\Gamma(p + k_2)\theta_2^p}{\Gamma(k_2)\Gamma(p + k_1)\theta_1^p}\right)^{-1}$$

We refer the reader to Appendix A.1 for the proof of Equation 7. In the anytime distribution, one of the components of the Gamma distribution will have an associated mixture coefficient $\varphi(p)$ or $1 - \varphi(p)$ which increases with p while the coefficient of the other component decreases proportionally. Note that for constant ($p = 0$) computational complexity, the anytime distribution is equal to the target distribution π .

5.1.1 Implementation

On a single processor, the Anytime Parallel Tempering Monte Carlo algorithm (referred to as APTMC-1) is implemented as follows: simulate $\Lambda = 8$ Markov chains, each targeting the distribution $\pi_\lambda(dx) = \pi(dx)^{\frac{\lambda}{\Lambda}}$. To construct a Markov chain $(X^\lambda)_{n=0}^\infty$ with target distribution

$$\pi_\lambda(x) \propto \left[\frac{1}{2} \text{Gamma}(k_1, \theta_1) + \frac{1}{2} \text{Gamma}(k_2, \theta_2)\right]^{\frac{\lambda}{\Lambda}}$$

for $\lambda = 1, \dots, \Lambda$, simply use a *Random Walk Metropolis* update, i.e. symmetric Gaussian proposal distribution $\mathcal{N}(x_n^\lambda, \sigma^2)$ with mean x_n^λ and standard deviation $\sigma = 0.5$. Set $(k_1, k_2) = (3, 20)$, $(\theta_1, \theta_2) = (0.15, 0.25)$ and use $p \in \{0, 1, 2, 3\}$. The single processor algorithm is run for $T = 10^8$ units of virtual time with exchange moves alternating between occurring on all even $(1, 2), (3, 4), (5, 6)$ and all odd $(2, 3), (4, 5), (6, 7)$ pairs of inactive chains every $\delta = 5$ time steps. When the algorithm is running, a sample is recorded every time a local or exchange move occurs.

On multiple processors, the APTMC algorithm (referred to as APTMC-W) is implemented similarly. A number of $W = \Lambda = 8$ processors is used, where each worker $w = \lambda$ contains $K = 2$ chains, all targeting the same π_λ for $\lambda = 1, \dots, \Lambda$. The multiple processor algorithm is run for $T = 10^7$ units of virtual time, with exchange moves alternating between occurring on all odd $(1, 2), (3, 4), (5, 6), (7, 8)$ and all even $(2, 3), (4, 5), (6, 7)$ pairs of workers every $\delta = 5$ steps. On each worker, the chain which was not working when calculations were interrupted is the one included in the exchange moves.

5.1.2 Verification of bias correction

To check that the single and multiple processor algorithms are successfully correcting for bias, they are also run *uncorrected*, i.e. not excluding the currently working chain. This means that several exchange moves are performed on samples distributed according to α instead of π , thus causing the algorithm to yield biased results. Since the bias is introduced by the exchange moves (when they are performed on α), we attempt to create a ‘worst case scenario’, i.e. maximise the amount of bias present when the single processor algorithm is uncorrected. The algorithm is further adjusted such that local moves are not performed on the cold chain and it is instead solely made up of samples resulting from exchange moves with the warmer chains. The fact that exchange moves occur every $\delta = 5$ units of virtual time also means that a high proportion of the samples in a warmer chain come from exchange moves. The multi-processor APTMC-W algorithm is not run in a ‘worst case scenario’, so local moves on the cold chain of the multi-processor algorithm are therefore allowed. This means that the bias caused by failing to correct when performing exchange moves across workers is still apparent, if less strongly.

Figure 3 shows kernel density estimates of the post burn-in cold chains resulting from runs of the APTMC-1 and APTMC-W algorithms, uncorrected and corrected for bias. As expected, when the hold time does not depend on x , which corresponds to the case there $p = 0$, no bias is returned. On the other hand, the cold chains for the single-processor algorithm with computational complexity $p \in \{1, 2, 3\}$ have clearly been corrupted by biased samples and converged to a shifted distribution which puts more weight the second Gamma mixture component, instead of an equal weight. Additionally, the bias becomes stronger as computational complexity p increases. A similar observation can be made for the cold chains from the multi-processor experiment – which display a milder bias due to local moves occurring on the cold chain. The green dashed densities indicate that when the algorithms are corrected, i.e. when the currently working chain is not included in exchange moves, it successfully eliminates the bias for all $p \in \{1, 2, 3\}$ to return the correct posterior π – despite even this being the ‘worst case scenario’ in the case of the APTMC-1 algorithm. Note that the uncorrected density estimates do not exactly correspond to the anytime distributions. This has nothing to do with burn-in, but with the proportion of biased samples (from exchange moves) present in the chain.

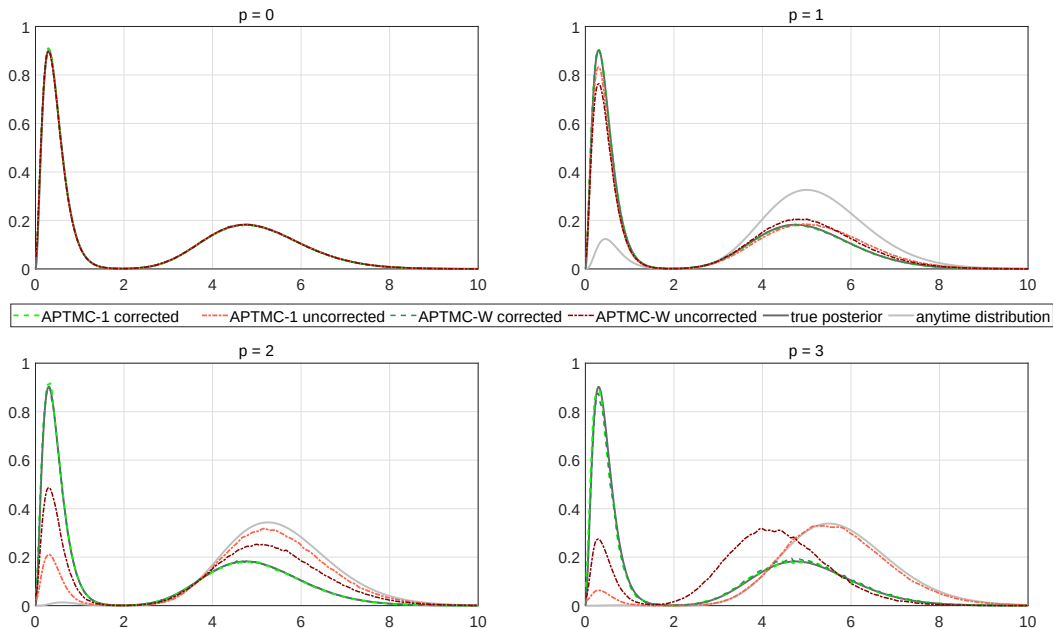


Figure 3: Density estimates of the cold chain for bias corrected and uncorrected runs of the single (APTMC-1) and multi-processor (APTMC-W) algorithms on various hold time distributions $p \in \{0, 1, 2, 3\}$. In the single-processor case, the cold chain is made up entirely of updates resulting from exchange moves. The solid *dark grey* line represents the true posterior density π and the solid *light grey* line the anytime distribution α . The case $p = 0$ represents an instance in which, in a real-time situation, the local moves do not take a random time to complete, and therefore all densities are identical. The two *green* dashed lines represent bias corrected densities and the *red* dot-dashed represent uncorrected densities. For $p \geq 1$, the two corrected densities are identical to the posterior, indicating that the bias correction was successful.

5.1.3 Performance evaluation

Next we verify that introducing the parallel tempering element to the Anytime Monte Carlo algorithm improves performance. A standard MCMC algorithm is run for computational complexities $p \in \{0, 1, 2, 3\}$, applying the random walk Metropolis update described in Section 5.1.1. The single and multiple processor APTMC algorithms are run again for the same amount of virtual time, with exchange moves occurring every $\delta_{0:2} = 5$ units of virtual time for $p \leq 2$ and every $\delta_3 = 30$ units when $p = 3$. The single processor version is run on $\Lambda_s = 8$ chains, and the multi-processor on $W = 8$ workers, with $K = 2$ chains per worker, so $\Lambda_m = 16$ chains in total. This time, local moves are performed on the cold chain of the single processor APTMC-1 algorithm.

To compare results, kernel density estimates of the posterior are obtained from the post burn-in cold chains for each algorithm using the `kde` function in [MATLAB \[2019\]](#), developed by [Botev et al. \[2010\]](#). It is also important to note that even though all algorithms run for the same (virtual) duration, the standard MCMC algorithm is performing local moves on a single chain uninterrupted until the deadline, while the APTMC-1 algorithm has to update $\Lambda = 8$ chains in sequence, and each worker w of the APTMC- W algorithm has to update $K = 2$ chains in sequence before exchange moves occur. Therefore, by time T the algorithms will not have returned samples of similar sizes. For a fair performance comparison, the sample autocorrelation function (acf) is estimated first of all. When available, the acf is averaged over multiple chains to reduce variance in its estimates. Other tools employed are

- *Integrated Autocorrelation Time (IAT)*, the computational inefficiency of a MCMC sampler. Defined as

$$IAT_s = 1 + 2 \sum_{\ell=1}^{\infty} \rho_s(\ell)$$

where $\rho_s(\ell)$ is the autocorrelation at the ℓ -th lag of chain s . It measures the average number of iterations required for an independent sample to be drawn, or in other words the number of correlated samples with same variance as one independent sample. Hence, a more efficient algorithm will have lower autocorrelation values and should yield a lower *IAT* value. Here, the *IAT* is estimated using a method initially suggested in [Sokal \[1997\]](#) and [Goodman and Weare \[2010\]](#), and implemented in the Python package `emcee` by [Foreman-Mackey et al. \[2013\]](#) (Section 3). Let

$$I\hat{A}T_s = 1 + 2 \sum_{\ell=1}^M \hat{\rho}_s(\ell)$$

where M is a suitably chosen cutoff, such that noise at the higher lags is reduced. Here, the smallest M is chosen such that $M \geq C \hat{\rho}_s(M)$ where $C \approx 6$. More information on the choice of C is available in [Sokal \[1997\]](#).

- *Effective Sample Size (ESS)*, the amount of information obtained from a MCMC sample. It is closely linked to the *IAT* by definition:

$$ESS_s = \frac{N_s}{IAT_s}$$

where N_s is the size of the current sample s . The *ESS* measures the number of independent samples obtained from MCMC output.

The resulting *ESS* and *IAT* for different algorithms and computational complexities are computed and shown in Table 1. If an exchange move is accepted, the new state of the chain does not

depend on the value of the previous state. This means that the autocorrelation in a chain containing a significant proportion of (accepted) samples originating from exchange moves will be lower. For low p , significantly more local moves occur before each deadline, as hold times are short, while for a higher p , the hold times are longer and hence fewer local moves are able to occur. Therefore, higher values of p will yield a higher proportion of samples from exchange moves, and thus a more notable increase in efficiency.

5.1.4 Performance results

In Figure 4 we observe, unsurprisingly, that the quality of the posterior estimates decreases as p increases. As a matter of fact, 10^7 units of virtual time tend to not be enough for the some of the posterior chains to completely converge. Indeed, while the standard MCMC algorithm performs reasonably well for $p = 0$, it becomes increasingly harder for it to fully converge for higher computational complexities. Similarly, the single processor APTMC-1 algorithm returns reasonably accurate posterior estimates for $p \leq 2$ but then visibly underestimates the first mode of the true posterior for $p = 3$. In general, the multi-processor APTMC-W algorithm returns results closest to the true cold posterior for all p .

As for efficiency, Table 1 displays a much lower *IAT* and much higher *ESS* for both APTMC algorithms, indicating that they are much more efficient than the standard MCMC algorithm. This is further supported by the sample autocorrelation decaying much more quickly for APTMC algorithms than for the MCMC algorithm for all p in Figure 5. The multi-processor APTMC-W algorithm also yields *IAT* values that are lower than those returned by the single processor APTMC-1 algorithm for $p < 3$, and similarly yields effective sample sizes that are higher for all p . The *ESS* and *IAT* values for chains that have not converged to their posterior have been omitted from the table.

p	Multi-processor		Single-processor		Standard	
	APTMC-W		APTMC-1		MCMC	
	<i>IAT</i>	<i>ESS</i>	<i>IAT</i>	<i>ESS</i>	<i>IAT</i>	<i>ESS</i>
0	53.925	12049	81.156	1202.2	1739.0	287.46
1	45.942	5888.3	95.104	708.74	2818.2	64.047
2	80.871	1168.4	132.79	448.92	-	-
3	131.91	116.51	-	-	-	-

Table 1: Integrated autocorrelation time (*IAT*) and effective sample size (*ESS*) for runs of the single, multi-processor Anytime parallel tempering and standard MCMC algorithms. The algorithms were run for 10^6 units of virtual time for computational complexity $p = 0$ and 10^7 units for $p \geq 1$, and the resulting *ESSs* were scaled down for consistency with $p = 0$. The *ESS* and *IAT* values for chains that have not converged to their posterior have been omitted.

Next, we consider an application of the APTMC framework to approximate Bayesian computation, a class of algorithms that are well-adapted to situations in which the likelihood is either intractable or computationally prohibitive. Approximate Bayesian Computation features a real hold time at each MCMC iteration, making it an ideal candidate for adaptation to the Anytime parallel tempering framework.

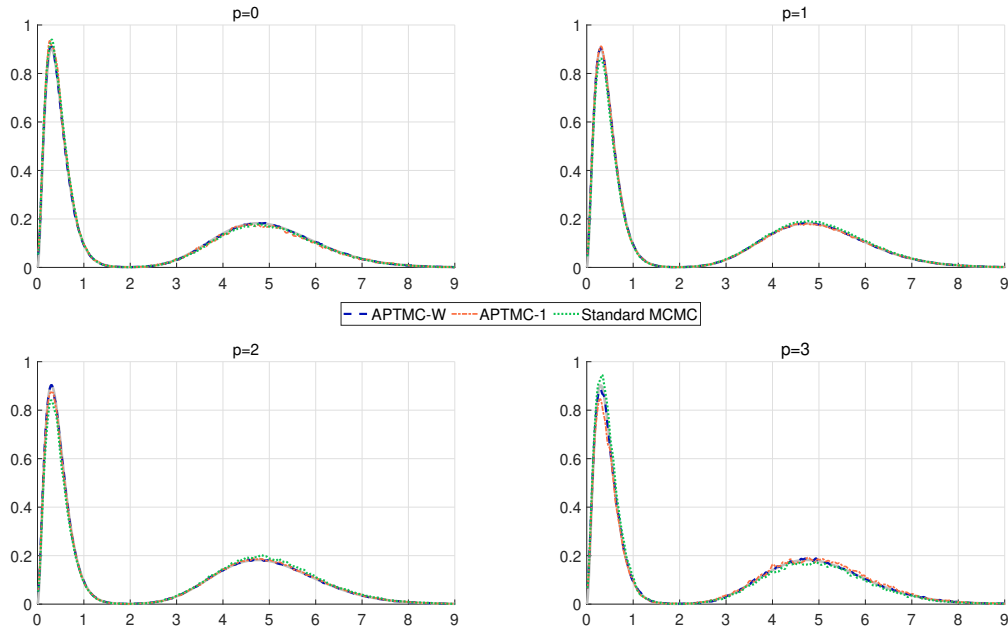


Figure 4: Density estimates of the cold posterior for runs of the single (*orange*) and multiple (*blue*) processor APTMC algorithms (APTMC-1 and APTMC-W, respectively) as well as the standard (*green*) MCMC algorithm. The *grey* line represents the true posterior density π . Each plot corresponds to a different hold time distribution $p \in \{0, 1, 2, 3\}$. While the multi processor density has successfully converged for all p – as evidenced by the perfect overlap between the grey and dark blue lines –, the other two algorithms tend to struggle more and more to estimate the first mode of the posterior as p increases.

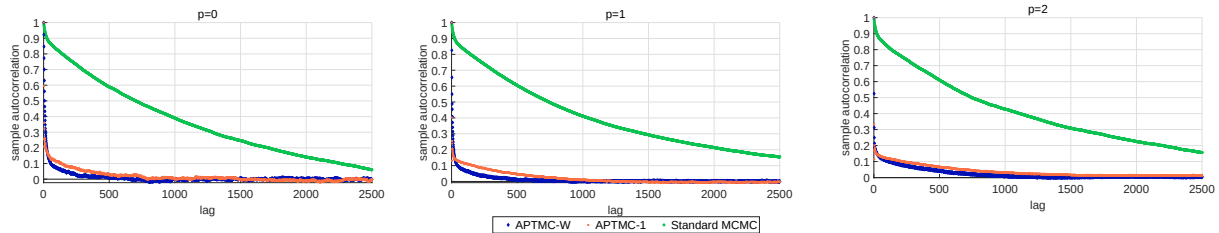


Figure 5: Plots of the sample autocorrelation function up to lag 2500 of the post burn-in cold chain for runs of the single (*orange*) and multiple (*blue*) processor APTMC algorithms (APTMC-1 and APTMC-W, respectively) as well as for the output of the standard Anytime Monte Carlo (MCMC) algorithm (*green*). Each plot corresponds to a different computational complexity $p \in \{0, 1, 2\}$. The two APTMC algorithms clearly perform considerably better than standard MCMC for all p . The sample acf plot for $p = 3$ has been omitted due to both the APTMC and MCMC chains not having fully converged to their posterior.

5.2 ABC toy example: univariate Normal distribution

To validate the results of Section 4.2, consider another simple example, initially featured in Lee [2012], and adapted here within the APTMC framework. Let Y be a Gaussian random variable, i.e. $Y \sim \mathcal{N}(y; \theta, \sigma^2)$, where the standard deviation σ is known but the mean θ is not. The approximate Bayesian computation likelihood here is

$$f^\varepsilon(y | \theta) = \Phi\left(\frac{y + \varepsilon - \theta}{\sigma}\right) - \Phi\left(\frac{y - \varepsilon - \theta}{\sigma}\right)$$

for $\varepsilon > 0$ where $\Phi(\cdot)$ is the cumulative distribution function (cdf) of a standard Gaussian. Using numerical integration tools in MATLAB, it is possible to obtain a good approximation of the true posterior for any ε for visualisation. Let $y = 3$ be an observation of Y and $\sigma^2 = 1$, and put the prior $p(\theta) = \mathcal{N}(\theta; 0, 5)$ on θ . In this example, the exact posterior distribution for θ can easily be shown to be $\mathcal{N}(\theta; \frac{5}{2}, \frac{5}{6})$.

When performing local moves (Algorithm 3), use a Gaussian random walk proposal with standard deviation $\xi = 0.5$. The real-time Markov jump process is run using $\Lambda = 10$ chains. The algorithm is run on a single processor for one hour or $T = 3600$ seconds in real time after a 30 second burn-in, with exchange moves occurring every $\delta_T = 5 \times 10^{-4}$ seconds (or 0.5 milliseconds). The radii of the balls $\varepsilon^{1:\Lambda}$ are defined to vary between $\varepsilon^1 = 0.1$ and $\varepsilon^\Lambda = 1.1$.

We verify that bias correction must be applied for all chains to converge to the correct posterior. This is done by comparing density estimates of each of the post burn-in chains to the true corresponding posterior (obtained by numerical integration). When bias correction is not applied, the ABC-APTMC algorithm does not exclude the currently working chain j in its exchange moves. In this case, every chain converges to an erroneous distribution which overestimates the mode of its corresponding posterior, as is clearly visible in Figure 6. On the other hand, correcting the algorithm for such bias ensures that every chain converges to the correct corresponding posterior.

Next, we compare the performance of the ABC-APTMC algorithm to that of a standard approximate Bayesian computation (referred to as standard ABC) algorithm. For that, a more applied parameter estimation example is considered, for which the adoption of a likelihood-free approach is necessary.

5.3 Stochastic Lotka-Volterra model

In this section, we consider the stochastic Lotka-Volterra predator-prey model (Lotka [1926], Volterra [1927]), further exploring the example considered in Lee and Łatuszyński [2014], which is itself based on an example in Chapter 6 of Wilkinson [2011]. In this case study, the posterior is intractable and some of the components of the parameters θ (namely θ_2 and θ_3) exhibit strong correlations. Let $X_{1:2}(t)$ be a bivariate, integer-valued pure jump Markov process with initial values $X_{1:2}(0) = (50, 100)$, where $X_1(t)$ represents the number of preys and $X_2(t)$ the number of predators at time t . For small time interval Δt , we describe the predator-prey dynamics in the following way:

$$\mathbb{P}\{X_{1:2}(t + \Delta t) = z_{1:2} | X_{1:2}(t) = x_{1:2}\} = \begin{cases} \theta_1 x_1 \Delta t + o(\Delta t), & \text{if } z_{1:2} = (x_1 + 1, x_2) \\ \theta_2 x_1 x_2 \Delta t + o(\Delta t), & \text{if } z_{1:2} = (x_1 - 1, x_2 + 1) \\ \theta_3 x_2 \Delta t + o(\Delta t), & \text{if } z_{1:2} = (x_1, x_2 - 1) \\ o(\Delta t), & \text{otherwise} \end{cases}$$

In this example, the only observations available are the number of preys, i.e. X_1 at 10 discrete time points. Following theory in Wilkinson [2011] (Chapter 6), the process can be simulated and

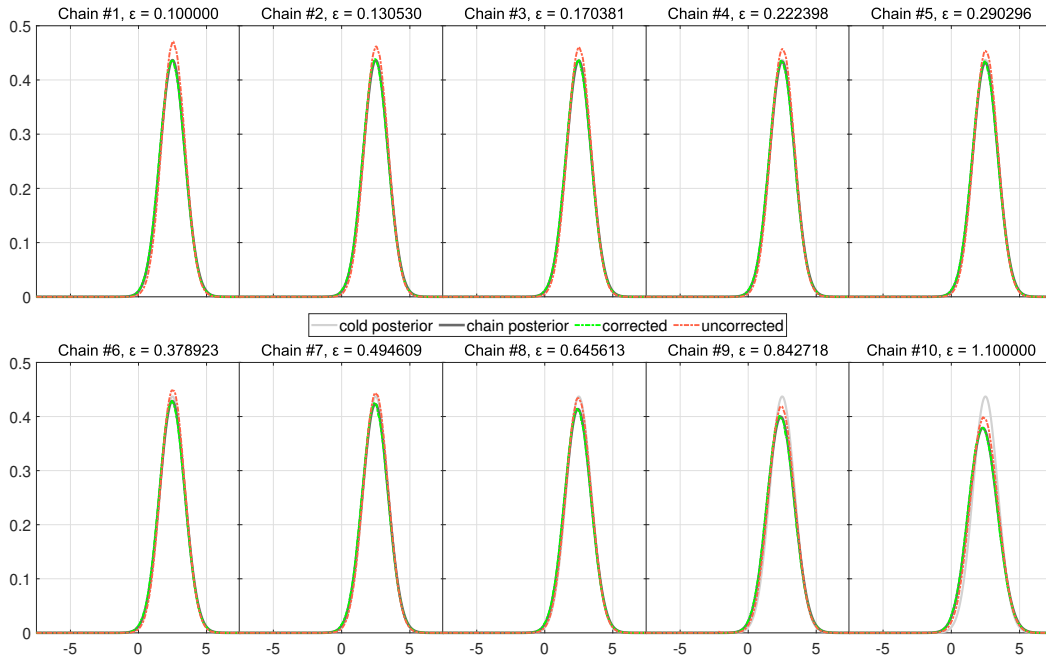


Figure 6: Kernel density estimates of all chains for corrected and uncorrected runs of the single processor ABC-APTMC algorithm. In each subplot, the *light grey* line is fixed and represents the cold posterior for reference, the *dark grey* line represents each chain’s target posterior (obtained by numerical integration), the dot-dashed *green* lines are kernel density estimates of the chain’s posterior returned by the corrected algorithm and are indistinguishable from the dark grey line. The *orange* lines are kernel density estimates for the uncorrected algorithm, and do not agree with the dark grey line, as expected.

discretised using the Gillespie [1977] algorithm, in which the inter-jump times follow an exponential distribution. The observations employed were simulated in Lee and Łatuszyński [2014] with true parameters $\theta = (1, 0.005, 0.6)$, giving $y = \{88, 165, 274, 268, 114, 46, 32, 36, 53, 92\}$ at times $\{1, \dots, 10\}$. For approximate Bayesian computation, the ‘ball’ considered takes the following form for $\varepsilon > 0$

$$B_\varepsilon(y) = \{X_1(t) : |\log [X_1(i)] - \log [y(i)]| \leq \varepsilon, \forall i = 1, \dots, 10\} \quad (8)$$

therefore, a set of simulated $X_1(t)$ is considered as ‘hitting the ball’ if all 10 simulated data points are at most e^ε times (and at least $e^{-\varepsilon}$ times) the magnitude of the corresponding observation in y .

5.3.1 Methods and settings

In Lee and Łatuszyński [2014] (Algorithm 3), the 1-hit MCMC kernel (referred to in experiments as standard ABC), is shown to return the most reliable results by comparison with other MCMC kernels which are not considered here. While it can be reasonably fast, it is highly inefficient as it has a very low acceptance rate, and thus the autocorrelation between samples for low lags is very high. We have established that the race step in Algorithm 3 takes a random time complete. In addition to that, its hold time distribution for the Lotka-Volterra model is a mixture between quick and lengthy completion times, as the simulation steps within the 1-hit kernel race are capable of taking a considerable amount of time despite often being almost instant. Indeed, when simulating observations using the discretised Gillespie algorithm, if the number of predators is low, prey numbers will flourish and the simulation will take longer. Hence another important issue in this particular model is that the race can sometimes get stuck for extended periods of time if the number of preys to simulate is especially high. Therefore, we aim to first of all improve performances by introducing exchange moves on a single processor (ABC-PTMC). Then – and most importantly – we further improve the algorithm by implementing it within the Anytime framework (ABC-APTMC), a method which works especially well on multiple processors.

5.3.1.1 One processor

The first part of this case study is run on a single processor and serves to demonstrate the gain in efficiency introduced by the exchange moves described in Algorithm 4. Departing slightly from the example in Lee and Łatuszyński [2014], define the prior on $\theta \in [0, \infty)^3$ for the single processor experiment to be $p(\theta) = \exp\{-\theta_1 - \theta_2 - \theta_3\}$, i.e. three independent exponential priors, all with mean 1. The proposal distribution is a truncated normal, i.e. $\theta' | \theta \sim \mathcal{TN}(\theta, \Sigma)$, $\theta' \in (0, 10)$ with mean θ and covariance $\Sigma = \text{diag}(0.25, 0.0025, 0.25)$. The truncated normal is used in order to ensure that all proposals remain non-negative. For reference, 2364 independent samples from the posterior are obtained via approximate Bayesian computation rejection sampling with $\varepsilon = 1$ and the density estimates in Figure 6 of Lee and Łatuszyński [2014] are reproduced. To obtain these posterior samples, 10^7 independent samples from the prior were required, yielding the very low 0.024% acceptance rate. This method of sampling from the posterior is therefore extremely inefficient, and the decision to resort to MCMC kernels in order to improve efficiency is justified.

On a single processor, the three algorithms considered are the vanilla 1-hit MCMC kernel (standard ABC) defined in Algorithm 3, the single processor version of the algorithm with added exchange moves (ABC-PTMC-1) and the same but within the Anytime framework (ABC-APTMC-1). They are run nine times for 100800 seconds (28 hours) – after 3600 seconds (1 hour) of burn-in – and their main settings are summarised in Table 2. It is also important to note that the parallel tempering algorithms, having to deal with updating multiple chains sequentially, are likely

to return cold chains with fewer samples. The algorithms must therefore be properly set up such that the gain in efficiency introduced by exchange moves is not overshadowed by the greater number of chains and computational cost of having to update them all. In this experiment, the parallel tempering algorithms are run on 6 chains, each targeting posteriors associated with balls of radii $\varepsilon^{1:6} = \{1, 1.1447, 1.3104, 1.5, 11, 15\}$ and the proposal distribution has covariance $\Sigma^{1:6}$ where $\Sigma^\lambda = \text{diag}(\sigma^\lambda, \sigma^\lambda 10^{-2}, \sigma^\lambda)$ and $\sigma^{1:6} = \{0.008, 0.025, 0.05, 0.09, 0.25, 0.5\}$. Exchange moves are performed as described in Algorithm 4 and alternate between odd (1, 2), (3, 4), (5, 6) (excluding (5, 6) in the Anytime version) and even (2, 3), (4, 5) pairs of eligible chains. In the Anytime (ABC-APTMC-1) version, in order to determine how long the local moves should run for before exchange moves occur, the time taken for the standard ABC-PTMC-1 algorithm to perform a fixed number δ_T of local moves is measured at each iteration, and the median over all iterations is taken. This ensures that both algorithms spend the same median time performing local moves.

<i>Label</i>	<i>Workers</i> <i>W</i>	<i>Chains</i> <i>K</i>	<i>Chains per</i> <i>worker</i>	<i>Exchange moves</i> <i>(every)</i>	<i>Anytime</i>
ABC	1	1	1	none	No
ABC-PTMC-1	1	6	6	6 local moves	No
ABC-APTMC-1	1	6	6	2.59 seconds	Yes

Table 2: Algorithm information and settings for stochastic Lotka-Volterra predator-prey model on a single processor.

5.3.1.2 Multiple processors

Now, we aim to demonstrate the gain in efficiency introduced by running the parallel tempering algorithm within the Anytime framework on multiple processors. The algorithms considered are the multi-processor ABC-PTMC-*W* and ABC-APTMC-*W* algorithms and their single processor counterparts ABC-PTMC-1 and ABC-APTMC-1. This time, instead of relying on an informative, exponential prior on θ , we define a uniform prior between 0 and 3. The proposal distribution is still a truncated normal, but with tighter limits (corresponding to the prior) i.e. $\theta' | \theta \sim TN(\theta, \Sigma)$, $\theta' \in (0, 3)$. Again, 1988 independent samples from the posterior are obtained for reference. They are generated via approximate Bayesian computation rejection sampling with $\varepsilon = 1$. To obtain these posterior samples, 10^8 independent samples from the prior were required, yielding the even lower 0.002% acceptance rate.

The two algorithms are run on 20 chains, each targeting posteriors associated with balls of radii ranging from $\varepsilon^1 = 1$ to $\varepsilon^{20} = 11$ and proposal distribution covariances $\Sigma^{1:21}$ where $\Sigma^k = \text{diag}(\sigma^k, \sigma^k 10^{-2}, \sigma^k)$ for chain k and where values range from $\sigma^1 = 0.008$ to $\sigma^{20} = 0.5$. These are tuned so that the acceptance rates of exchange moves between adjacent chains remain on average greater than 70%. The algorithms are run four times for 864000 seconds (24 hours) and their main settings are summarised in Table 3.

In this experiment, multiple chains running at different temperatures are present on each worker. In order to account for the approximately 1 second communication overhead when switching between local moves – running in parallel on all workers – and exchange moves – running on the master –, exchange moves are divided into two types:

1. Exchange moves *within workers*: performed on each individual worker in parallel, between a pair of adjacent chains selected at random. No communication between workers is necessary

<i>Label</i>	<i>Workers</i> <i>W</i>	<i>Chains</i> <i>K</i>	<i>Chains per</i> <i>worker</i>	<i>Communication</i> <i>overhead</i>	<i>Exchange moves (every)</i>	<i>Anytime</i>
ABC-PTMC-1	1	20	20	-	20 local moves	No
ABC-APTMC-1	1	20	20	-	11 seconds	Yes
ABC-PTMC-W	4	20	5	1.1 seconds	5 local moves	No
ABC-APTMC-W	4	20	5	1.1 seconds	5 local moves (<i>within</i> workers) 15.3 seconds (<i>between</i> workers)	Yes

Table 3: Algorithm information and settings for stochastic Lotka-Volterra predator-prey model on multiple processors.

in this case.

2. Exchange moves *between workers*: performed on the master by selecting a pair of adjacent workers at random and exchanging between the warmest eligible chain from the first worker and coldest from the second. Thus, an exchange move between two adjacent chains is effectively being performed, except this time communication between workers is required.

We now describe how the hard deadline for the ABC-APTMC-W algorithm is selected. In this new algorithm construction, the time (excluding communication overhead) taken for the ABC-PTMC-W algorithm to perform a set of parallel updates – i.e. δ_T local moves, an exchange move within workers and δ_T more local moves – is measured on each worker and at each iteration. Then, the median over all iterations is taken for each worker, and the hard deadline for parallel updates for the ABC-APTMC-W algorithm is set to be the median time the slowest of all workers took in the run of the ABC-PTMC-W algorithm. This ensures that all workers have a chance to perform the δ_T local moves.

5.3.2 Performance evaluation

All algorithms returned density estimates that were reasonably close to those obtained via rejection sampling. In order to compare the performance of the algorithms, as stated above, all algorithms compared are set to run for the same real time period. Once again the integrated autocorrelation time (*IAT*) and effective sample size (*ESS*) are computed for all algorithms. While the *IAT* and sample autocorrelation plots are good tools for comparing efficiency, they do not take into account the computational cost of running 6 chains instead of a single one. The *ESS* on the other hand gives us how many effective samples the different algorithms can return within a fixed time frame. For example, a very fast algorithm could still return a higher *ESS* even if it has a much higher *IAT*. To illustrate how the Anytime version of the parallel tempering algorithms works compared to standard ABC-PTMC, the real times all algorithms take to perform local and exchange moves are measured and their timelines plotted in Figure 8.

5.3.2.1 One processor

Both the ABC-PTMC-1 and ABC-APTMC-1 algorithm display an improvement in performances: they return *IAT*s that are respectively 3.2 and 1.6 times lower on average than those of the standard ABC algorithm in Table 4, and display a steeper decay in sample autocorrelation in Figure 7. In the 28 hours (post burn-in) during which the algorithms ran, both parallel algorithms also yielded an increased effective sample size. The effect of the Anytime framework on the behaviour of the parallel tempering algorithm is demonstrated in Figure 8. The timeline of local moves for the ABC-PTMC-1

algorithm illustrates the fact that local moves take a random amount of time to complete. This is mitigated since a deadline was implemented in the Anytime version of the algorithm. As a result, the bottom plot in Figure 8 displays more consistent local move times.

Note that in Table 4, while the improvement in IAT is significant, the increase in ESS after 28 hours is not particularly huge. This is due to the previously mentioned erratic behaviour of the hold time distribution for this example. Other examples explored such as the moving average example in Marin et al. [2012] (not reported here) yielded a much more significant increase in ESS after introducing exchange moves. We also note that in this example, the ABC-PTMC-1 algorithm returned a lower IAT than its Anytime counterpart. This is due to two reasons. The first reason is that Anytime algorithms cannot always exchange the samples of adjacent chains, because they must exclude the chain that is currently computing; this causes a slightly higher rejection rate compared to the standard version (in the multi-processor example with more chains, this is mitigated). The second reason is once again the erratic hold time distribution: while one chain is stuck for a long period, exchange moves are still occurring on all other chains, but they are attempting to swap the same five values of θ among each other. The strength of the Anytime framework is best illustrated in a multi-processor setting.

The single processor experiment was mainly designed to demonstrate the performance improvements brought by adding exchange moves to the 1-hit MCMC kernel (referred to as standard ABC). Indeed, while the Anytime framework is capable of improving effective sample size, it is not at its most useful on a single processor, as it is subject to the same obstacles as its standard counterpart. It is on multiple processors that the benefits of the Anytime framework become especially apparent.

	Standard ABC		ABC-PTMC-1		ABC-APTMC-1	
	IAT	ESS	IAT	ESS	IAT	ESS
θ_1	69.476	7018.1	22.404	7618.6	44.071	7963.8
θ_2	122.73	3973	35.381	4824.2	69.803	5028
θ_3	150.74	3234.6	50.035	3411.3	98.929	3547.7

Table 4: Effective sample size (ESS) and integrated autocorrelation time (IAT) over nine 28-hour runs of the standard ABC, ABC-PTMC-1 and ABC-APTMC-1 algorithms to estimate the posterior distributions of the parameters $\theta = (\theta_1, \theta_2, \theta_3)$ of a stochastic Lotka-Volterra model. Improvements in performance are modest in this example.

5.3.2.2 Multiple processors

In the multi-processor case study, both the ABC-PTMC-1 and ABC-PTMC-W were set so that on each worker, an exchange move occurred after all chains had been updated locally once, as described in Table 3. The total number of samples returned by the ABC-PTMC-W algorithm is higher for all chains (see Table 6) and therefore the approximately 1.1 second communication overhead was not prohibitive. However, the ABC-PTMC-W algorithm is just as affected by the distribution of the hold times being a mixture of quick and lengthy completion times as its single processor counterpart, and is just as prone to getting stuck in a race for an extended period. During this time, all processors sit idle while waiting for the race to complete, as illustrated in Figure 9. Therefore, the ABC-PTMC-W algorithm struggles to properly boost the total sample size output by the cold chain, and the ESS is not markedly higher on average in Table 5. On the other hand, thanks to the real time deadlines

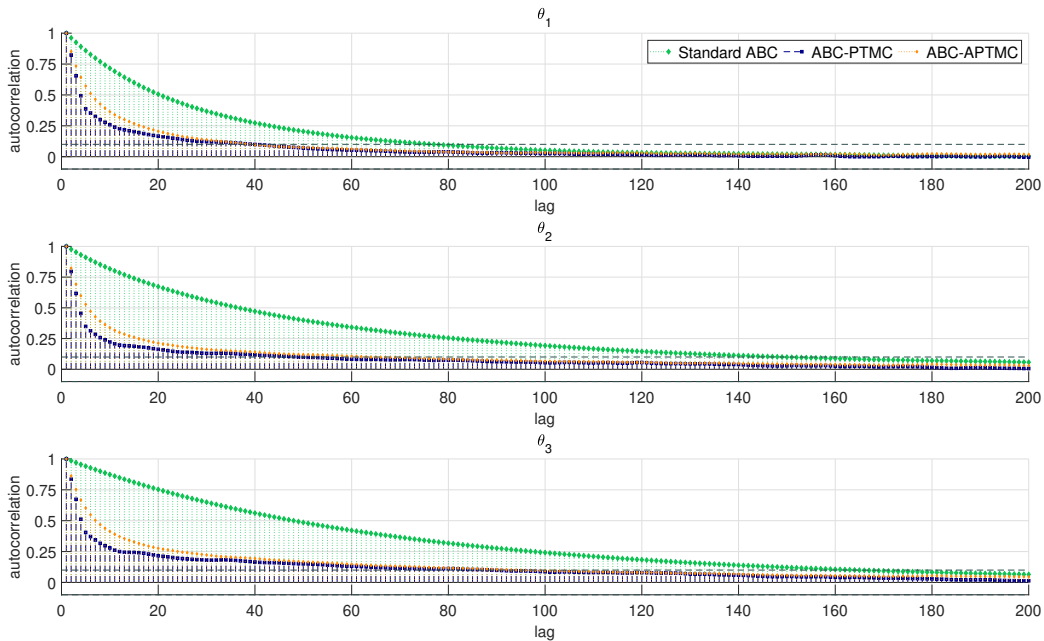


Figure 7: Plots of the sample autocorrelation function up to lag 200 of the cold chain for runs of the standard ABC (*green*), ABC-PTMC-1 (*blue*) and ABC-APTMC-1 (*orange*) algorithms to estimate the posterior distributions of the parameters $\theta = (\theta_1, \theta_2, \theta_3)$ of a stochastic Lotka-Volterra model. The inclusion of exchange moves boosts efficiency and leads to a steeper decay in the parallel tempering algorithms.

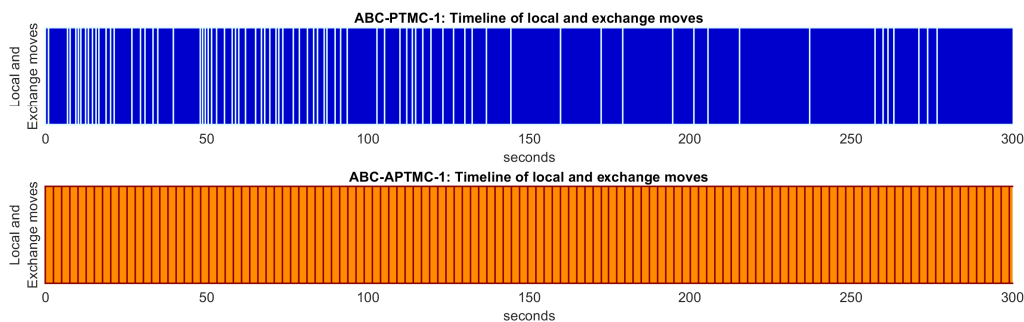


Figure 8: Timeline of local and exchange moves for the ABC-PTMC-1 and ABC-APTMC-1 algorithms for the first 300 seconds. The exchange moves are represented by the *white* and *red* lines and the local moves by the *dark blue* and *orange* coloured blocks. Local moves take a random amount of time to complete, as illustrated by the times consumed by local moves for the ABC-PTMC-1 algorithm. The Anytime (ABC-APTMC-1) version effectively implements a hard deadline for the exchange moves (without introducing a bias), as can be seen by the regularity of local move times in the bottom figure.

implemented, the ABC-APTMC-W algorithm is able to more than double the total size of the samples output (see Table 6), and the effective sample sizes for the cold chain returned in Table 5 are on average 3.41 times higher than those of the single processor version.

As for the main comparison – namely Anytime vs standard approximate Bayesian computation with exchange moves – both single and multi-processor Anytime algorithms return an effective sample larger than their respective standard versions in Table 5. While the improvement on a single processor is not huge, the *ESS* has more than quadrupled on multiple processors. Figures 9 and 10 illustrate well the advantage of implementing a real-time deadline to local moves. At most local moves, the issue in which all workers sit idle waiting for the slowest to finish arises for the ABC-PTMC-W algorithm. On the other hand, Figure 10 clearly shows that the Anytime version of the algorithm is making better use of the allocated computational resources. The Anytime framework ensures that none of the workers need to wait for the slowest among them to finish, allowing for more exploration of the sample space in the faster workers. Additionally, the real time deadline ensures that even if chain k on Worker w remains stuck in a race for an extended period of time, the other workers are still updating. Therefore, while the remaining four chains on Worker w wait for chain k to complete its race, they also continue to be updated at regular intervals thanks to the exchange moves with other workers.

	One processor				Multiple processors			
	ABC-PTMC-1		ABC-APTMC-1		ABC-PTMC-W		ABC-APTMC-W	
	<i>IAT</i>	<i>ESS</i>	<i>IAT</i>	<i>ESS</i>	<i>IAT</i>	<i>ESS</i>	<i>IAT</i>	<i>ESS</i>
θ_1	39.535	269.89	72.475	362.62	48.621	266.7	39.898	1452.5
θ_2	72.908	146.35	88.446	297.14	67.395	192.4	72.79	796.14
θ_3	82.464	129.39	138.56	189.68	87.635	147.97	101.57	570.57

Table 5: Effective sample size (*ESS*) and integrated autocorrelation time (*IAT*) over four 24-hour runs of the ABC-PTMC-1, ABC-APTMC-1, ABC-PTMC-W and ABC-APTMC-W algorithms to estimate the posterior distributions of the parameters $\theta = (\theta_1, \theta_2, \theta_3)$ of a stochastic Lotka-Volterra model.

The addition of approximate Bayesian computation exchange moves in his case study proved fruitful, as the effective sample size for the parameters of the Lotka-Volterra model was increased. However this required fine tuning of the settings. The benefits of approximate Bayesian computation parallel tempering will be stronger and more easily visible in a problem in which the parameters to be estimated have a multimodal distribution, as a single chain may get stuck in local optima while multiple tempered chains will explore more of the sample space. Nonetheless, the introduction of the Anytime framework is clearly an important improvement. It ensures the various chains in approximate Bayesian computation parallel tempering continue to be updated (via exchange moves) even when one of them is stuck performing local moves for longer than expected, and encourages the algorithm to make better use of its allocated resources on multiple processors.

6 Conclusion

In an effort to increase the efficiency of MCMC algorithms, in particular for use on multiple processors, and for situations in which the likelihood is unavailable and/or compute times of the algorithms depend on their current states, the Anytime Parallel Tempering Monte Carlo (APTMC) algorithm

was developed. The algorithm combines the enhanced exploration of the state space, provided by the between-chain exchange moves in parallel tempering, with control over the real-time budget and robustness to interruptions available within the Anytime Monte Carlo framework.

Initially, the construction of the Anytime Monte Carlo algorithm with the inclusion of exchange moves on a single and multiple processors was verified on a toy Gamma mixture example. The performance improvements they brought were then demonstrated by comparing the algorithm to a standard MCMC algorithm. Subsequently, the exchange moves were adapted for pairing with the 1-hit MCMC kernel, a simulation-based algorithm within approximate Bayesian computation framework, which provides an attractive, likelihood-free approach to MCMC. The construction of the adapted approximate Bayesian computation algorithm was verified using a simple univariate normal example. Then, the increased efficiency of the inclusion of exchange moves was demonstrated in comparison to that of a standard approximate Bayesian computation algorithm on a parameter estimation problem. The problem involved the parameters of a stochastic Lotka-Volterra predator-prey model based on partial and discrete data, and the likelihood of this model is intractable. On a single processor, it was shown that introducing exchange moves provides an improvement in performance and an increase in the effective sample size compared to that of the standard, single chain approximate Bayesian computation algorithm. On multiple processors, it was shown that the Anytime framework helps the parallel tempering approximate Bayesian computation algorithm to make more efficient use of the computational resources and thus provides a strong boost to effective sample size.

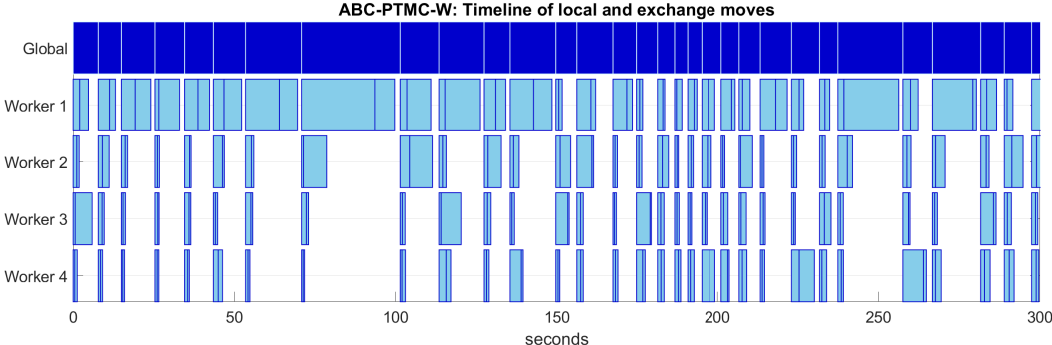


Figure 9: Timeline of local and exchange moves for the ABC-PTMC-W algorithm for the first 300 seconds. Within and between worker exchange moves are represented by the *white lines* on the Global timeline and *blue lines* on the various Worker timelines, respectively. Local moves on each worker are represented by the *light blue* coloured blocks and the *dark blue* coloured blocks correspond to the global time all workers spend running in parallel, including communication overhead. Significant idle time is apparent on all workers as they always have to wait for the slowest among them to complete its set of local moves.

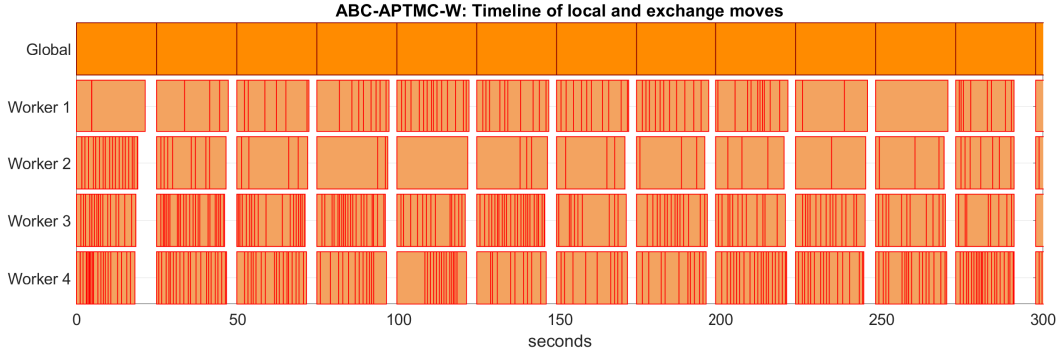


Figure 10: Timeline of local and exchange moves for the ABC-APTMC-W algorithm for the first 300 seconds. Within and between worker exchange moves are represented by the *red lines*. Local moves on each worker are represented by the various *orange* coloured blocks, with the brighter blocks corresponding to the global time all workers spend running in parallel, including communication overhead. The significant idle time from Figure 9 has been greatly reduced thanks to the deadlines implemented.

Chain k	ε^k	σ^k	ABC-PTMC-1	ABC-PTMC-W	ABC-APTMC-1	ABC-APTMC-W
1	1	0.008	2667.5	3241.8	6570.3	14488
2	1.046	0.009	2790	3564.8	6934.8	16902
3	1.094	0.011	2796.8	3567.5	6941	16837
4	1.145	0.012	2797.3	3604.5	6924.8	17264
5	1.197	0.014	2793.8	3719.8	6931.3	15710
6	1.253	0.016	2786.3	3748.8	6951.5	17157
7	1.31	0.019	2784.8	3629.3	6961.3	18947
8	1.371	0.022	2795.5	3615	6941.5	18551
9	1.434	0.025	2805.5	3608.5	6950.8	18759
10	1.5	0.029	2803.5	3711.5	6962.8	17276
11	1.661	0.034	2798.5	3799.8	6962.3	46350
12	1.84	0.039	2803.3	3693.3	6983	53716
13	2.038	0.045	2814.8	3656.5	6995.3	53289
14	2.257	0.052	2799	3658.3	7008.8	53458
15	2.5	0.06	2783.5	3796.3	7029.8	46597
16	3.362	0.092	2787.5	4054.5	7038.5	68953
17	4.522	0.14	2783.8	3936.5	7009.5	79231
18	6.082	0.214	2781	3912.5	6982.5	78917
19	8.179	0.327	2780.8	3919.5	7002.8	79038
20	11	0.5	2665.8	3598.5	6604.3	67725

Table 6: Average sample sizes per chain returned over four 24-hour runs of the ABC-PTMC-1, ABC-APTMC-1, ABC-PTMC-W, ABC-APTMC-W algorithms to estimate the posterior distributions of the parameters θ of a stochastic Lotka-Volterra model on multiple processors in Section 5.3.2. The ball radius ε^k and proposal distribution covariance $\text{diag}(\sigma^k, \sigma^k 10^{-2}, \sigma^k)$ associated with each chain k are displayed for information.

References

- A. Beskos, G. Roberts, A. Stuart, et al. Optimal scalings for local Metropolis–Hastings chains on nonproduct targets in high dimensions. *The Annals of Applied Probability*, 19(3):863–898, 2009.
- Z. I. Botev, J. F. Grotowski, D. P. Kroese, et al. Kernel density estimation via diffusion. *The Annals of Statistics*, 38(5):2916–2957, 2010.
- D. Foreman-Mackey, D. W. Hogg, D. Lang, and J. Goodman. emcee: The MCMC Hammer. *Publications of the Astronomical Society of the Pacific*, 125(925):306, 2013.
- C. Geyer. Importance sampling, simulated tempering and umbrella sampling. *Handbook of Markov Chain Monte Carlo*, pages 295–311, 2011.
- C. J. Geyer. Markov chain Monte Carlo maximum likelihood. *Interface Foundation of North America*, 1991.
- D. T. Gillespie. Exact stochastic simulation of coupled chemical reactions. *The journal of physical chemistry*, 81(25):2340–2361, 1977.
- J. Goodman and J. Weare. Ensemble samplers with affine invariance. *Communications in applied mathematics and computational science*, 5(1):65–80, 2010.
- A. Lee. On the choice of MCMC kernels for approximate Bayesian computation with SMC samplers. In *Simulation Conference (WSC), Proceedings of the 2012 Winter*, pages 1–12. IEEE, 2012.
- A. Lee and K. Łatuszyński. Variance bounding and geometric ergodicity of markov chain monte carlo kernels for approximate bayesian computation. *Biometrika*, 101(3):655–671, 2014.
- A. J. Lotka. Elements of Physical Biology. *Science Progress in the Twentieth Century (1919-1933)*, 21(82):341–343, 1926.
- J.-M. Marin, P. Pudlo, C. P. Robert, and R. J. Ryder. Approximate Bayesian computational methods. *Statistics and Computing*, pages 1–14, 2012.
- MATLAB. *version 9.7.0.1190202 (R2019b)*. The MathWorks Inc., Natick, Massachusetts, 2019.
- L. M. Murray, S. Singh, P. E. Jacob, and A. Lee. Anytime Monte Carlo. *arXiv preprint arXiv:1612.03319*, 2016. URL <https://arxiv.org/abs/1612.03319>.
- J. K. Pritchard, M. T. Seielstad, A. Perez-Lezaun, and M. W. Feldman. Population growth of human Y chromosomes: a study of Y chromosome microsatellites. *Molecular biology and evolution*, 16(12):1791–1798, 1999.
- C. Robert and G. Casella. *Monte Carlo Statistical Methods*, chapter The Metropolis-Hastings Algorithm. Springer Texts in Statistics, Springer, New York, 2004. ISBN 978-1-4757-4145-2. doi: 10.1007/978-1-4757-4145-2_7.
- A. Sokal. Monte Carlo Methods in Statistical Mechanics: Foundations and New Algorithms. In *Functional integration*, pages 131–192. Springer, 1997.
- R. H. Swendsen and J.-S. Wang. Replica Monte Carlo simulation of spin-glasses. *Physical Review Letters*, 57(21):2607, 1986.

S. Tavaré, D. J. Balding, R. C. Griffiths, and P. Donnelly. Inferring coalescence times from DNA sequence data. *Genetics*, 145(2):505–518, 1997.

V. Volterra. *Variazioni e fluttuazioni del numero d'individui in specie animali conviventi*. C. Ferrari, 1927.

D. J. Wilkinson. *Stochastic Modelling for Systems Biology*. CRC press, 2011.

A Proofs

A.1 Anytime distribution of the cold chain

To obtain the anytime distribution in the Gamma mixture example in Section 5.1, compute the three components of the expression in Equation (4):

1. The density of X

$$\pi(dx) = \frac{x^{k_1-1}}{2\Gamma(k_1)\theta_1^{k_1}} e^{-\frac{x}{\theta_1}} + \frac{x^{k_2-1}}{2\Gamma(k_2)\theta_2^{k_2}} e^{-\frac{x}{\theta_2}} dx$$

where $\Gamma(\cdot)$ is the gamma function.

2. The expectation of $H | x$ given by

$$\mathbb{E}[H | x] = \psi x^p + (1 - \psi)x^p = x^p$$

The ψ factors cancel out, meaning that the anytime distribution is independent of ψ and therefore its value can be chosen to be 1 for convenience.

3. To compute $\mathbb{E}[H]$, use a property of conditional expectation and the honesty conditions of the $\text{Gamma}(k_1 + p, \theta_1)$ and $\text{Gamma}(k_2 + p, \theta_2)$ distributions:

$$\begin{aligned} \mathbb{E}[H] &= \mathbb{E}[\mathbb{E}(H | x)] = \mathbb{E}[x^p] \\ &= \int \frac{x^{p+k_1-1}}{2\Gamma(k_1)\theta_1^{k_1}} e^{-\frac{x}{\theta_1}} dx + \int \frac{x^{p+k_2-1}}{2\Gamma(k_2)\theta_2^{k_2}} e^{-\frac{x}{\theta_2}} dx \\ &= \frac{\Gamma(k_2)\Gamma(p+k_1)\theta_1^p + \Gamma(k_1)\Gamma(p+k_2)\theta_2^p}{2\Gamma(k_1)\Gamma(k_2)} \\ &= \frac{C}{2\Gamma(k_1)\Gamma(k_2)} \end{aligned}$$

letting $C = \Gamma(k_2)\Gamma(p+k_1)\theta_1^p + \Gamma(k_1)\Gamma(p+k_2)\theta_2^p$.

Combining the three components,

$$\begin{aligned} \alpha(dx) &= \frac{2\Gamma(k_1)\Gamma(k_2)}{C} \left(\frac{x^{p+k_1-1}}{2\Gamma(k_1)\theta_1^{k_1}} e^{-\frac{x}{\theta_1}} + \frac{x^{p+k_2-1}}{2\Gamma(k_2)\theta_2^{k_2}} e^{-\frac{x}{\theta_2}} \right) dx \\ &= \underbrace{\frac{\Gamma(k_2)\Gamma(p+k_1)\theta_1^{p+k_1}}{C\theta_1^{k_1}}}_{\varphi(p,k_1,k_2,\theta_1,\theta_2)} \underbrace{\frac{x^{p+k_1-1}}{\Gamma(p+k_1)\theta_1^{p+k_1}} e^{-\frac{x}{\theta_1}}}_{\text{Gamma}(p+k_1,\theta_1)} + \underbrace{\frac{\Gamma(k_1)\Gamma(p+k_2)\theta_2^{p+k_2}}{C\theta_2^{k_2}}}_{\varphi'(p,k_1,k_2,\theta_1,\theta_2)} \underbrace{\frac{x^{p+k_2-1}}{\Gamma(p+k_2)\theta_2^{p+k_2}} e^{-\frac{x}{\theta_2}}}_{\text{Gamma}(p+k_2,\theta_2)} dx \end{aligned}$$

And now substituting back the expression C in φ :

$$\varphi(p, k_1, k_2, \theta_1, \theta_2) = \frac{1}{1 + \frac{\Gamma(k_1)\Gamma(p+k_2)\theta_2^p}{\Gamma(k_2)\Gamma(p+k_1)\theta_1^p}}$$

Similarly, we can obtain $\varphi'(p, k_1, k_2, \theta_1, \theta_2) = 1 - \varphi(p, k_1, k_2, \theta_1, \theta_2)$. Therefore, the anytime distribution $\alpha(dx)$ is the following mixture of two Gamma distributions:

$$\alpha(dx) = \varphi(p, k_1, k_2, \theta_1, \theta_2) \text{Gamma}(k_1 + p, \theta_1) + (1 - \varphi(p, k_1, k_2, \theta_1, \theta_2)) \text{Gamma}(k_2 + p, \theta_2)$$